Spectroscopic Characterization and Reactivity of Triplet and Quintet Iron(IV) Oxo Complexes in the Gas Phase

Erik Andris, Juraj Jašík, Laura Gómez, Miquel Costas,* and Jana Roithová*

Abstract: *Closely structurally related triplet and quintet iron-(IV) oxo complexes with a tetradentate aminopyridine ligand were generated in the gas phase, spectroscopically characterized, and their reactivities in hydrogen-transfer and oxygen-transfer reactions were compared. The spin states were unambiguously assigned based on helium tagging infrared photodissociation (IRPD) spectra of the mass-selected iron complexes. It is shown that the stretching vibrations of the nitrate counterion can be used as a spectral marker of the central iron spin state.*

The search for reagents capable of selectively oxidizing an alkane C−H bond, and characterization of their chemistry are actively pursued and challenging goals in modern synthesis. One of the most promising approaches is based on hypervalent transition-metal oxo complexes.[1,2] An important advantage of using transition metals and their oxo complexes is the potential they offer to explore multistate reactivity.[3–6] Metal oxo complexes with a high-spin ground state are usually considered to be more reactive,[7–10] but also low-spin highly reactive complexes were reported.[11] Direct comparison of the reactivities of high-spin and low-spin

complexes has not been reported so far because only one type of the given complex, the more stable one, is usually prepared.[7]

The genuine reactivity of clearly defined complexes can be directly compared in the gas phase[12–16] and it can enlighten the role of spin in the reactivity of metal oxo complexes. It is necessary, however, to develop a method for characterization of the spin-states of such mass-selected complexes in the gas phase. Herein, we present a spectroscopic characterization of iron(IV) oxo complexes with a tetradentate ligand denoted as PyTACN (PyTACN = 1-[2′-(pyridyl)methyl]-4,7-dimethyl-1,4,7-triazacyclononane, Scheme 1) in the triplet ($S=1$) as well as the quintet ($S=2$) state.
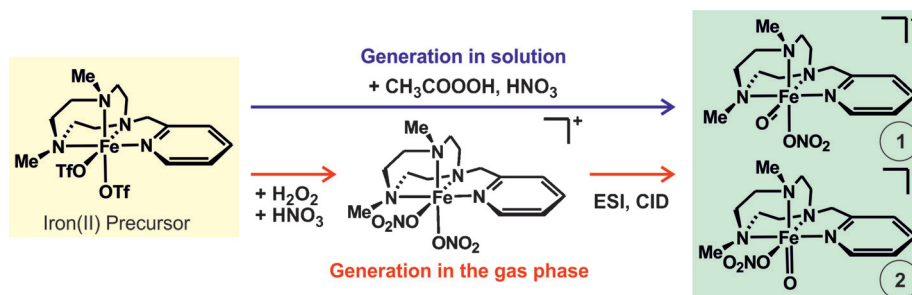
Scheme 1. Generation of [(PyTACN)Fe(O)(NO₃)]⁺ by oxidation of the iron(II) precursor in solution or by in-source CID during electrospray ionization.

The reactive ions were formed in acetonitrile solution from their iron(II) precursor [(PyTACN)Fe(OTf)₂] by oxidation with peracetic acid. Mössbauer spectroscopy has demonstrated that this reaction sequence leads to the generation of triplet state iron(IV) complexes ($S=1$).[17] Using electrospray ionization (ESI) we were able to transfer the [(PyTACN)Fe(O)(OTf)]⁺ ions to the gas phase and on addition of HNO₃, the [(PyTACN)Fe(O)(NO₃)]⁺ ions (m/z 382) were also detected (Figure S5 in the Supporting Information). Alternatively, in the gas phase, hypervalent metal oxo complexes can be generated by radical cleavage of the nitrate counterions (i.e. M-ONO₂ fragments to M-O• and NO₂•).[18] To generate complexes analogous to those of the condensed phase, the [(PyTACN)Fe(OTf)₂] precursor was oxidized by H₂O₂ to the corresponding iron(III) complex. In the presence of HNO₃, the abundant [(PyTACN)Fe(NO₃)₂]⁺ complexes were detected by ESI-MS. Collisional activation of these complexes led to elimination of NO₂• radicals and the generation of the desired [(PyTACN)Fe(O)(NO₃)]⁺ complexes (Figures S4 and S5).

We have analyzed the structures and spin states of the gaseous [(PyTACN)Fe(O)(NO₃)]⁺ complexes by helium tag-

[*] E. Andris, J. Jašík, Prof. J. Roithová
Department of Organic Chemistry
Faculty of Science, Charles University in Prague
Hlavova 2030/8, 12843 Prague 2 (Czech Republic)
E-mail: roithova@natur.cuni.cz

Dr. L. Gómez, Prof. M. Costas
Departament de Quimica and Institute of Computational Chemistry and Catalysis (IQCC), University of Girona
Campus Montilivi, Girona 17071 (Spain)
E-mail: miquel.costas@udg.edu

Dr. L. Gómez
Serveis Tècnics de Recerca (STR), Universitat de Girona
Parc Científic i Tecnològic, 17003 Girona (Spain)

Supporting information and the ORCID identification number(s) for the author(s) of this article can be found under http://dx.doi.org/10.1002/anie.201511374.

ging infrared photodissociation (IRPD) spectroscopy.[19] The complexes were generated either by the oxidation in solution and transferred to the gas phase by ESI, or by in-source fragmentation during ESI of the iron(III) nitrate precursor complexes. The mass-selected complexes are trapped in a cryo-cooled ion trap (2.5 K) with helium buffer gas and form $[(PyTACN)Fe(O)(NO_3)(He)]^+$ complexes.[20] Helium atoms serve as swift leaving tags where an increase of the complexes internal energy results in their dissociation.[21] Monitoring helium elimination from the tagged complexes can be thus used to sensitively detect the absorption of IR photons. Dependence of the depletion of the helium complex on the wavenumber of incident IR photons provides IRPD spectra of the complexes.[22]

Comparison of the IRPD spectra of the complexes generated in solution and in the gas phase reveals distinct differences in the range of the nitrate antisymmetric stretching mode (bands around 1590 cm⁻¹) and around 900 cm⁻¹ (Figure 1a). To assign the individual peaks, we have studied the range from 1540 cm⁻¹ to 1640 cm⁻¹ by two-color IRPD spectroscopy (Figure 1b and Figure S10) of the ions gener-

ated in the gas phase.[23] The spectra clearly show that we are working with two distinct groups of ions. The major group is characterized by the peaks at 1582 cm⁻¹ and 1603 cm⁻¹, whereas the band at 1570 cm⁻¹ belongs to the other group. The helium complexes from the first group are depleted by irradiation of the ion cloud at 1603 cm⁻¹. The spectrum generated by subsequent probing with a second photon beam (black line in Figure 1b) resembles that of the ions generated in solution (blue line in Figure 1b). Under the assumption that the experimental IRPD spectra result from a linear combination of the spectra of two species, we have extracted the corresponding base spectra (Figure 1c). They can be linearly combined in a 0.75:0.25 ratio to provide the IRPD spectrum of the ions transferred from the oxidized solution, and in a 0.35:0.65 ratio to provide the IRPD spectrum of ions obtained by in-source fragmentation (Figure S11). Note that the ratios are reversed, so the ions characterized by the blue spectrum in Figure 1c are mostly formed by the oxidation in solution, whereas the ions characterized by the pink spectrum in Figure 1c are mostly formed by in-source fragmentation of the iron(III) precursors. We were not able to completely suppress the in-source fragmentation of the iron(III) precursors, therefore it also partly contributed to the ions formed by in-solution oxidation.

Interpretation of the IRPD spectra is based on comparison with theoretical IR spectra of possible isomers for the $[(PyTACN)Fe(O)(NO_3)]^+$ complex (Figure 1d). We have assumed that the oxygen atom can either be in plane with the pyridine (equatorial position) or perpendicular to the plane of the pyridine (axial position; isomers **1** and **2** in Scheme 1, green panel). Both isomers can be present either in the triplet state or the quintet state. We have performed a series of DFT calculations. It can be stated that the correct ordering of the spin states cannot be reliably determined by DFT methods (Figure 2). While the PBEPBE functional energetically largely favors the triplet states of both isomers, B3LYP predicts ³**1** as the most stable isomer followed by ⁵**2**. The OPBE functional predicts ⁵**2** as the most stable species and
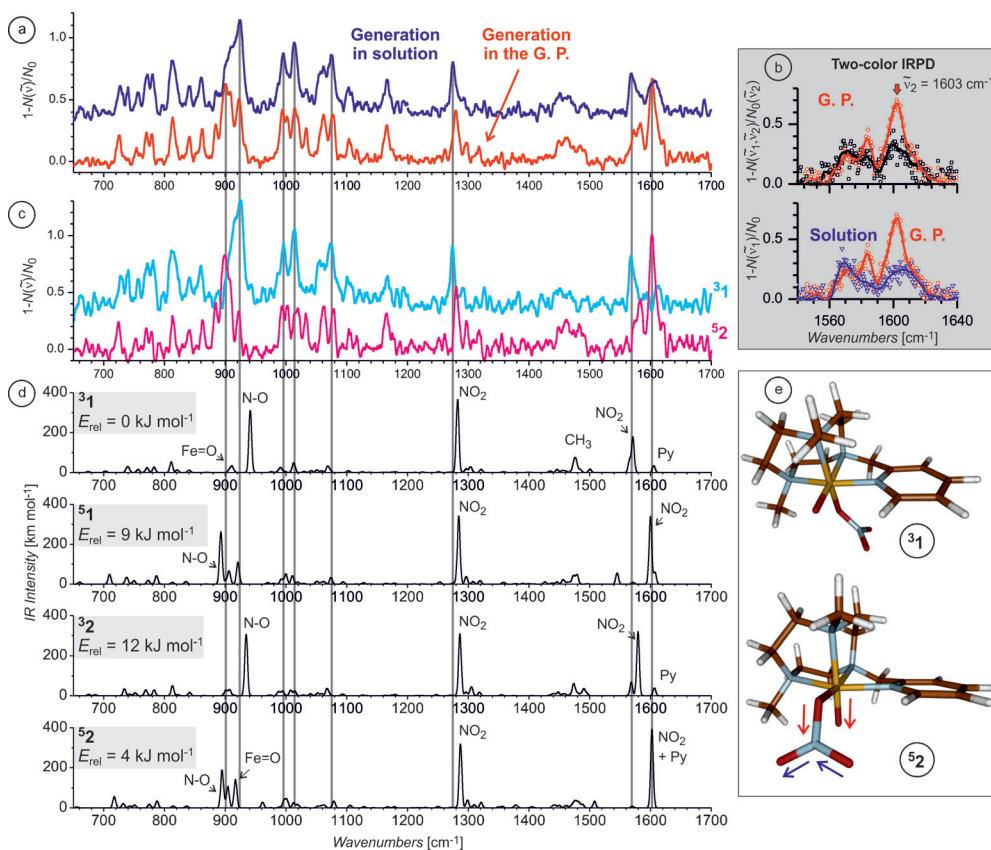

Figure 1. a) IRPD spectra of $[(PyTACN)Fe(O)(NO_3)]^+$ (m/z 382) generated by oxidation in solution (blue trace, shifted on the y-scale by 0.4 for clarity) or by in-source collisional activation during ESI (red trace) G.P. = gas phase. b) Top panel: Two-color IRPD experiment with the ions generated in the gas phase, one optical paramagnetic oscillator (OPO) was set to 1603 cm⁻¹, the second OPO was scanned (black trace). Lower panel shows one-color IRPD spectra from (a) in detail. c) Separated spectra of the two complexes contributing to the IRPD spectra shown in (a). The spectra are normalized to the original N_0. d) Theoretical IR spectra of ³**1**, ⁵**1**, ³**2**, and ⁵**2** calculated with B3LYP-D3/6-311++G**. e) The most stable structures of ³**1** and ⁵**2**. The red arrows denote the NO and FeO stretching vibrations responsible for the bands at around 900 cm⁻¹ and the blue arrows show the antisymmetric stretch of the NO_2 group, located at about 1600 cm⁻¹.
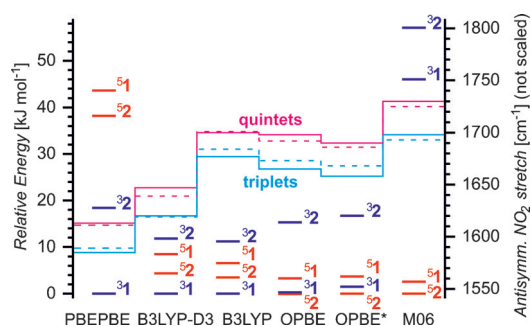
Figure 2. Results of DFT calculations (the functionals are specified at the bottom of the data, the basis set was always 6-311++G**, for the OPBE functional also def2-TZVP was tested—denoted by asterisk). The red and blue lines denote relative energies of the isomers (left axis); the pink and light blue lines show the unscaled antisymmetric NO_2 stretch for quintet and triplet states, respectively (dashed lines are for the **1** isomers and solid lines are for the **2** isomers).

finally the M06 functional largely stabilizes both quintet states with respect to the triplet states (results obtained with other DFT functionals can be found in the Supporting Information, Figures S14, S15, Table S3). It should be stressed that not only the ordering of the spin states is changing in dependence of the used DFT functional, but also optimized geometries of triplet and quintet states differ and favor the particular state. The correct theoretical treatment thus not only requires high-level multi-reference calculations but also full geometry optimizations at the given level are necessary.

Contrary to the energy assignments, the IR characteristics of the given spin-isomers are predicted consistently and can be used for the assignment of the ions studied experimentally. The antisymmetric stretching of the NO_2 unit (cf. Figure 1e) is blue-shifted for the quintet states with respect to the triplet states (pink vs. light blue line in Figure 2). Natural bond orbital (NBO) analysis shows that there is consistently greater spin localization at the nitrate counterions for the quintet states which is reflected in the blue shift of the antisymmetric NO_2 stretch (Table S3). Another effect observed for the quintet-state complexes is a red shift of the N−O vibration below 900 cm^{-1} (cf. Figure 1d,e). Analogous band shifts are also observed experimentally. Hence, the ions generated in the gas phase by in-source fragmentation reveal a blue-shifted band at 1603 cm^{-1} and a red-shifted band at 900 cm^{-1} with respect to the bands observed for the ions obtained by oxidation in solution. Therefore we conclude that the ions generated by in-source fragmentation of the iron(III) precursors are in the quintet state (^{5}**1** and/or ^{5}**2**). The ions oxidized by peracetic acid in solution and transferred to the gas phase are then triplets (^{3}**1** and/or ^{3}**2**). Note that this is in agreement with the previous results obtained by Mössbauer spectroscopy.[17]

The expected Fe=O stretch is predicted in the computed spectra of ^{3}**1**, ^{5}**1**, ^{3}**2**, and ^{5}**2** at approximately 900 cm^{-1}. These are commonly low-intensity vibrational features and cannot be discerned in the experimental IRPD spectra. They are blue shifted with respect to the value obtained by resonance Raman spectroscopy for [(PyTACN)Fe(O)(CH$_3$CN)]$^{2+}$ in

frozen acetonitrile solution (831 cm^{-1}).[17] The experimentally determined Fe=O stretches of iron(IV) complexes in condensed phase expand from 780 to 900 cm^{-1} and a spin correlation with the spin state cannot be established.[24]

The IRPD spectra do not give strong evidence for which isomers are formed. Nevertheless, DFT methods are much more reliable in determination of relative stabilities of isomers than in the prediction of spin states.[25] We can state that all tested DFT methods predict that the ^{3}**1** isomer is substantially more stable than the ^{3}**2** isomer (at least 10 kJ mol^{-1}). Hence, we conclude that by electrospray ionization of the ions oxidized in solution we generate the ^{3}**1** isomers. Under the assumption that the spin-isomerization at the iron atom is fast,[3,5] it can be also concluded that the triplet state is the ground state of the isomer **1**. Significantly, **1** reproduces the spin and isomeric structure previously determined in acetonitrile solution.

For the quintet states, the ^{5}**2** isomer is consistently more stable than the equatorial ^{5}**1** isomer. The energy differences are smaller than those for the isomers in the triplet state (4 kJ mol^{-1} on average). Theoretically, we could thus generate, by in-source fragmentation, a mixture of both isomers ^{5}**1** and ^{5}**2**. Again, under the assumption that spin-isomerization at the iron atom is fast, the ^{5}**1** isomer is expected to cross over to the ^{3}**1** ground state. We are thus left with the conclusion that the ions in the quintet state generated by in-source fragmentation of the iron(III) precursors correspond to the ^{5}**2** ions. We note in passing that we have excluded interference from other isomers of the generated complexes such as those with an oxidized ligand (Figure S16, S17).

Analysis of the IRPD spectra thus suggests that we are studying a mixture of ^{3}**1** and ^{5}**2**. The separated IRPD spectra shown in Figure 1c characterize the triplet isomer ^{3}**1** (the blue spectrum) and the quintet isomer ^{5}**2** (the pink spectrum). The ratio of ^{3}**1** and ^{5}**2** among the ions transferred from the solution and among those formed by in-source fragmentation is 0.75:0.25 and 0.35:0.65, respectively, as determined from linear combinations of the spectra.

In the next step, we have compared the reactivities of the ions and extracted reaction rates associated with the triplet- and quintet-state complexes (Table S1 in the Supporting Information). The ^{3}**1** and ^{5}**2** complexes differ not only in spin, but also in the orientation of the oxo group with respect to the plane of the pyridine ring. It was previously shown that the orientation of the oxo ligand perpendicular to the plane of the pyridine ligand can contribute to its larger reactivity.[26] As we have shown experimentally, it also contributes to the stabilization of the high-spin state. It might be possible that these two effects are interconnected (for example via lowering of the high-spin energy barrier for a reaction). In both isomers, **1** and **2**, an aliphatic amine is *trans* to the oxo ligand, and therefore this aspect can be reasonably discarded to differentiate the reactivity between isomers.[27] It was reported that a change of the ligand *trans* to the oxo ligand from an aliphatic amine to pyridine can lead to differences in reactivities for isospin iron complexes of an order of magnitude.[25]

The reaction was investigated with 1,4-cyclohexadiene and with partially deuterated 1,4-cyclohexadiene-[D$_6$] with both methylene groups bearing one H and one D atom
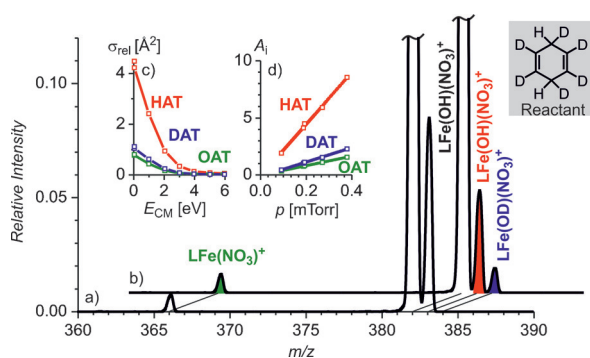
Figure 3. Mass spectra corresponding to the reaction of [(PyTACN)Fe-(O)(NO₃)]⁺ (*m/z* 382, these ions were generated by in-source fragmentation) with a) 1,4-cyclohexadiene and b) 1,4-cyclohexadiene-[D₆] (pressure of the neutral reactant was 0.2 mTorr). c) Collision-energy dependence (center-of-mass) of the cross-sections σ, and d) pressure dependence of the relative cross section *A* of HAT, DAT, and OAT in the reaction with 1,4-cyclohexadiene-[D₆] (*A*ᵢ is defined as −ln-(1−Σ*I*ₙ/(Σ*I*ₙ+*I*ₚ))(*I*ᵢ/Σ*I*ₙ), where *I*ₙ and *I*ₚ are intensities of the fragments and the parent, respectively). DAT = deuterium-atom transfer.

(Figure 3, Table S1). We have observed two reaction channels: i) Hydrogen-atom transfer (HAT) from the hydrocarbon to the iron(IV) complex detected as [(PyTACN)Fe(OH)-(NO₃)]⁺ (*m/z* 383, Figure 3a) and ii) Oxygen-atom transfer (OAT) from the complex to the hydrocarbon resulting in the [(PyTACN)Fe(NO₃)]⁺ signal (*m/z* 366). Both reaction channels are most efficient at zero collision energy as is expected for exothermic reactions proceeding via the formation of a collisional complex (e.g. Figure 3c).[28] Rate constants were determined from the pressure dependence of the relative reaction cross section (Figure 3d). The rate constant for the HAT (k_{HAT}) channel amounts to $(12 \pm 3) \times 10^{-12}$ cm³s⁻¹ with intramolecular kinetic isotope effect (KIE) of 4.07 ± 0.12 for the triplet-state complexes. For the quintet-state complexes, $k_{HAT} = (18.5 \pm 1.23) \times 10^{-12}$ cm³s⁻¹ with KIE = 4.13 ± 0.08. The KIE values suggest that the mechanism is not of a "harpoon" type for which KIE values lower than 2 would be expected.[29] Oxygen-transfer reaction is again slower for ³**1** with $k_{OAT} = (0.9 \pm 0.3) \times 10^{-12}$ cm³s⁻¹ than for ⁵**5** with $k_{OAT} = (1.61 \pm 0.13) \times 10^{-12}$ cm³s⁻¹. The rate constants for OAT did not change with deuterium labelling of the reactant, which demonstrates that we are observing an epoxidation reaction in the gas phase.

In summary, we show that helium-tagging infrared photodissociation spectroscopy can be used to distinguish triplet and quintet states of iron(IV) oxo complexes by shifts in stretching vibrations of nitrate counterions. It provides a powerful tool to characterize analogous reactive complexes in the gas phase and thus compare their reactivities. We demonstrate it herein for C−H activation and epoxidation reactions of iron(IV) oxo complexes with 1,4-cyclohexadiene. This opens a door for the systematic investigation of analogous triplet and quintet iron(IV) oxo complexes with different substrates and rationalize the reactivity trends in future.

[1] W. Nam, *Acc. Chem. Res.* **2015**, *48*, 2415–2423.
[2] M. Puri, L. Que, *Acc. Chem. Res.* **2015**, *48*, 2443–2452.
[3] H. Schwarz, *Int. J. Mass Spectrom.* **2004**, *237*, 75–105.
[4] D. Schröder, S. Shaik, H. Schwarz, *Acc. Chem. Res.* **2000**, *33*, 139–145.
[5] J. N. Harvey, R. Poli, K. M. Smith, *Coord. Chem. Rev.* **2003**, *238–239*, 347–361.
[6] S. Shaik, H. Hirao, D. Kumar, *Acc. Chem. Res.* **2007**, *40*, 532–542.
[7] K. P. Bryliakov, E. P. Talsi, *Coord. Chem. Rev.* **2014**, *276*, 73–96.
[8] S. Shaik, *Nat. Chem.* **2010**, *2*, 347–349.
[9] S. Shaik, H. Chen, D. Janardanan, *Nat. Chem.* **2011**, *3*, 19–27.
[10] D. Janardanan, Y. Wang, P. Schyman, L. Que, Jr., S. Shaik, *Angew. Chem. Int. Ed.* **2010**, *49*, 3342–3345; *Angew. Chem.* **2010**, *122*, 3414–3417.
[11] H. M. Neu, M. G. Quesne, T. S. Yang, K. A. Prokop-Prigge, K. M. Lancaster, J. Donohoe, S. DeBeer, S. P. de Visser, D. P. Goldberg, *Chem. Eur. J.* **2014**, *20*, 14584–14588.
[12] D. Schröder, H. Schwarz, *Proc. Natl. Acad. Sci. USA* **2008**, *105*, 18114–18119.
[13] W. A. Donald, C. J. McKenzie, R. A. J. O'Hair, *Angew. Chem. Int. Ed.* **2011**, *50*, 8379–8383; *Angew. Chem.* **2011**, *123*, 8529–8533.
[14] D. Schröder, H. Schwarz, N. Aliaga-Alcalde, F. Neese, *Eur. J. Inorg. Chem.* **2007**, 816–821.
[15] R. Mas-Ballesté, A. R. McDonald, D. Reed, D. Usharani, P. Schyman, P. Milko, S. Shaik, L. Que, Jr., *Chem. Eur. J.* **2012**, *18*, 11747–11760.
[16] M. A. Sainna, S. Kumar, D. Kumar, S. Fornarini, M. E. Crestoni, S. P. de Visser, *Chem. Sci.* **2015**, *6*, 1516–1529.
[17] A. Company, I. Prat, J. R. Frisch, R. M. Ballesté, M. Güell, G. Juhász, X. Ribas, E. Münck, J. M. Luis, L. Que, Jr., M. Costas, *Chem. Eur. J.* **2011**, *17*, 1622–1634.
[18] D. Schröder, J. Roithová, H. Schwarz, *Int. J. Mass Spectrom.* **2006**, *254*, 197–201.
[19] A. B. Wolk, C. M. Leavitt, E. Garand, M. A. Johnson, *Acc. Chem. Res.* **2014**, *47*, 202–210.
[20] J. Jašík, J. Žabka, J. Roithová, D. Gerlich, *Int. J. Mass Spectrom.* **2013**, *354–355*, 204–210.
[21] P. J. Kelleher, C. J. Johnson, J. A. Fournier, M. A. Johnson, A. B. McCoy, *J. Phys. Chem. A* **2015**, *119*, 4170–4176.
[22] J. Jašík, D. Gerlich, J. Roithová, *J. Am. Chem. Soc.* **2014**, *136*, 2960–2962.
[23] J. Jašík, D. Gerlich, J. Roithová, *J. Phys. Chem. A* **2015**, *119*, 2532–2542.

[24] A. R. McDonald, L. Que, Jr., *Coord. Chem. Rev.* **2013**, *257*, 414–428.

[25] S. Hong, Y.-M. Lee, K.-B. Cho, K. Sundaravel, J. Cho, M. J. Kim, W. Shin, W. Nam, *J. Am. Chem. Soc.* **2011**, *133*, 11876–11879.

[26] D. Wang, K. Ray, M. J. Collins, E. R. Farquhar, J. R. Frisch, L. Gomez, T. Jackson, M. Kerscher, A. Waleska, P. Comba, M. Costas, L. Que, Jr., *Chem. Sci.* **2013**, *4*, 282–291.

[27] S. P. de Visser, J.-U. Rohde, Y.-M. Lee, J. Cho, W. Nam, *Coord. Chem. Rev.* **2013**, *257*, 381–393.

[28] P. B. Armentrout, *Int. J. Mass Spectrom.* **2000**, *200*, 219–241.

[29] H. Schwarz, *Angew. Chem. Int. Ed.* **2011**, *50*, 10096–10115; *Angew. Chem.* **2011**, *123*, 10276–10297.